

Minerva Access is the Institutional Repository of The University of Melbourne

Author/s:

Dai, Q;Yan, Y;Guo, J;Björnmalm, M;Cui, J;Sun, H;Caruso, F

Title:

Targeting Ability of Affibody-Functionalized Particles Is Enhanced by Albumin but Inhibited by Serum Coronas

Date:

2015-10-30

Citation:

Dai, Q., Yan, Y., Guo, J., Björnmalm, M., Cui, J., Sun, H. & Caruso, F. (2015). Targeting Ability of Affibody-Functionalized Particles Is Enhanced by Albumin but Inhibited by Serum Coronas. *ACS Macro Letters*, 4 (11), pp.1259-1263. <https://doi.org/10.1021/acsmacrolett.5b00627>.

Persistent Link:

<https://hdl.handle.net/11343/90851>

# Targeting Ability of Affibody-Functionalized Particles is Enhanced by Albumin but Inhibited by Serum Coronas

Qiong Dai, Yan Yan, Junling Guo, Mattias Björnmalm, Jiwei Cui, Huanli Sun, and Frank Caruso\*

ARC Centre of Excellence in Convergent Bio-Nano Science and Technology, and the Department of Chemical and Biomolecular Engineering, The University of Melbourne, Parkville, Victoria 3010, Australia

---

**ABSTRACT:** Protein coronas formed on engineered particles can alter their targeting ability as they enter biological environments. Here, we engineer polymer coated silica particles and investigate the influence of protein coronas derived from various sources. The particles were functionalized with a small antibody-mimetic ligand (affibody), and their targeting ability to cancer cells in the presence of protein coronas was determined. Protein coronas derived from human serum showed a dramatic inhibition of specific particle-cell association (from ~70 to ~7%), whereas the most abundant protein in human serum—human serum albumin—enhanced the specific association of functionalized particles to SK-OV-3 human ovary cancer cells (to ~90%). This study shows how protein coronas can both facilitate and impede targeting and provides key insights into the importance of challenging engineered particles with multi-component biologically relevant environments.

---

Engineered particles functionalized with targeting ligands, such as transferrin,<sup>1</sup> folic acid,<sup>2</sup> and monoclonal antibodies,<sup>3</sup> have the potential to improve the delivery of a wide range of pharmaceutical agents toward specific types of cells or tissues. When particles enter biological environments, such as the blood stream, a layer of biomolecules adsorbs onto their surface with a large part of this layer being made up of proteins. This ‘protein corona’ is difficult to avoid and plays an important role in determining the ‘biological identity’ of the particles as well as impacting on their targeting ability.<sup>4,5</sup> There have been several studies that demonstrate the influence of protein coronas on the targeting ability of particle systems. For example, it has been shown that the deposition of proteins on silica nanoparticles shields alkyne groups from coupling with azide groups on a planar substrate.<sup>6</sup> The formation of protein coronas in cell culture media containing serum also resulted in a significant loss in the specificity of transferrin-functionalized silica nanoparticles.<sup>7</sup> Similarly, a considerable reduction in the targeting ability of single-domain antibody-functionalized silica nanoparticles in serum-containing media was observed.<sup>8</sup> However, monoclonal antibody-functionalized polymer particles retained their targeting ability in the presence of protein coronas derived from human serum (HS).<sup>9</sup> These studies highlight the important and different roles of protein coronas on the targeting ability of particle systems.

Human serum albumin (HSA), which constitutes about half of the blood serum proteins, is the most abundant protein in human blood plasma. With an extraordinary capacity of ligand binding, HSA is a main carrier for a series of compounds, such as fatty acids, thyroid hormones, bilirubin, and many exogenous drugs.<sup>10</sup> Further, HSA is well known to account for most of the antioxidant capacity of HS, affecting the pharmacokinetics of drugs, providing the metabolic modification of ligands, and rendering potential toxins harmless.<sup>10,11</sup> Thus, HSA has been an important model protein in the study of nano-bio interactions.<sup>12,13</sup> In particular, HSA has been used in fundamental studies of protein coronas formed on surfaces of nano-

particles, because it is present in the corona of virtually all nanoparticles studied.<sup>14-16</sup> Although these studies provide important insights into how HSA interacts with nanoparticles, how well they reflect what occurs in more complex biological environments (e.g., in serum, or in blood plasma) has not been extensively explored. The aim of this study was to systematically compare the influence of protein coronas on the properties of functionalized polymer particles, especially their targeting abilities, by using the single model protein, HSA, and the more biologically relevant HS, a widely used *in vitro* model.

A variety of targeting ligands, principally antibodies,<sup>3,17</sup> transferrin,<sup>18,19</sup> folate,<sup>20</sup> polypeptides,<sup>21,22</sup> DNA aptamers,<sup>23</sup> and carbohydrates,<sup>24</sup> have been employed to endow particles with targeting ability. Another class of targeting ligands that are of increasing interest is non-immunoglobulin-based affinity proteins.<sup>25,26</sup> A prominent example in this class, the affibody (Afb), is a small (~6 kDa), bacterially derived and recombinantly engineered protein affinity ligand.<sup>27</sup> Afb have been engineered to bind to a wide range of specific targets, e.g., the human epidermal growth factor receptor 2 (HER2), to which it has picomolar affinity.<sup>28</sup> The commercialized anti-HER2-Afb, with a recombinantly inserted C-terminal cysteine, binds to HER2 molecules overexpressed by certain cancer cells (e.g., SK-OV-3 human ovary cancer cells).<sup>29</sup> In the current work, alkyne-modified poly(methacrylic acid) (PMA<sub>alk</sub>, 8% modification, Figure S1) was used as a building block for the preparation of poly(methacrylic acid) (PMA)-coated silica particles (referred to as PMA particles in this study) assembled through the layer-by-layer (LbL) technique and copper(I)-catalyzed azide alkyne cycloaddition (CuAAC) chemistry (Figure S1).<sup>9,30</sup> The silica templates were 519 nm in diameter with assembled particles swelling to 1.0  $\mu\text{m}$  at physiological conditions. PMA particles were functionalized with the anti-HER2-Afb using a linear, bifunctional poly(ethylene glycol) (PEG) with a maleimide (reactive toward the cysteine on Afb) at one end and an azide (reactive toward the alkyne on particles via ‘click’ chemistry) at the other end (Mal-PEG-Az). The

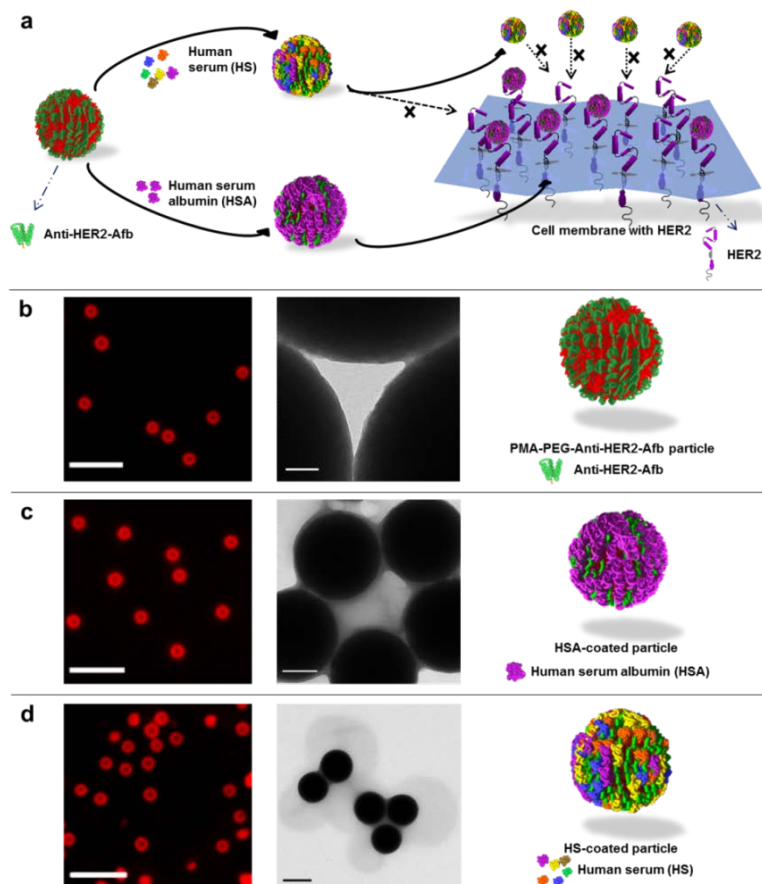


**Figure 1.** a) Schematic representation of the formation of different protein coronas on anti-HER2-Afb-functionalized PMA particles (PMA-PEG-Anti-HER2-Afb particles) exposed to HSA or HS, and the association of corona-coated particles with HER2 molecules on the cell membrane. b-d) Fluorescence microscopy images (left, scale bars are 5  $\mu\text{m}$ ), TEM images (middle, scale bars are 50 nm, 200 nm and 500 nm, respectively), and schematic representation of AF633-labeled (red) PMA-PEG-Anti-HER2-Afb particles without a protein corona (b) or with a protein corona derived from 20  $\text{mg mL}^{-1}$  HSA solution (c) and 100% HS (d).

coupling was qualitatively monitored by flow cytometry using a fluorescently labeled anti-Afb IgG (Figure S2). The increase of fluorescence intensity of particles incubated with anti-HER2-Afb (purple peak, Figure S2) compared with particles incubated with anti-HER2-Afb free buffer (black and red peak, Figure S2) clearly demonstrated the attachment of Afb onto the particle surface. The Afb-functionalized PMA particle system was then used to examine the influence of protein coronas (derived from various environments) on their targeting ability (Figure 1a).

Protein corona-coated particles were obtained by incubating the particles (Figure 1b) in various media (5, 10, 20  $\text{mg mL}^{-1}$  HSA or 10%, 50%, 100% (v/v) HS) followed by extensive washing to remove free proteins (10% HS contains  $\sim 5 \text{ mg mL}^{-1}$  HSA). The particles were well dispersed in aqueous solution without aggregation after HSA or HS coating (Figure 1c,d). A protein coating was clearly observed by transmission electron microscopy (TEM) for the particles incubated in 20  $\text{mg mL}^{-1}$  HSA solution or 100% HS (Figure 1c,d). The corona formed in 100% HS (as observed from the TEM images) is thicker than that formed in 20  $\text{mg mL}^{-1}$  HSA solution, which is expected, as there is a larger amount of protein in 100% HS (60-80  $\text{mg mL}^{-1}$  of total proteins and 30-50  $\text{mg mL}^{-1}$  of HSA).<sup>31</sup> Sodium dodecyl sulfate-polyacrylamide gel electrophoresis (SDS-PAGE) images also showed that a larger amount of protein adsorbed on particles when the concentration of protein

increased (Figure 2), which is in agreement with previously reported results.<sup>9</sup> Specifically, the total amount of protein adsorbed by particles in 10% HS (with a total protein concentration of 6-8  $\text{mg mL}^{-1}$ ) is lower than that adsorbed by particles in 20  $\text{mg mL}^{-1}$  HSA (Figure S3). These data revealed the protein concentration-dependent effects upon the adsorption of proteins on the surface of particles. However, the adsorption of proteins is influenced by a number of factors, such as the physicochemical properties of particles and other conditions (e.g., the solution concentration of salts).<sup>9</sup> Thus, the amount of protein adsorbed by particles is not in a linear correlation with the total amount of protein in the solution (Figure S3). There are various proteins, with HSA the most abundant one, in protein coronas derived from HS at various concentrations. This is expected because of the high abundance of HSA in serum.<sup>9,16</sup>

The targeting ability of these corona-coated particles was assessed in vitro. PMA-PEG-Anti-HER2-Afb particles without or with a protein corona derived from either 20  $\text{mg mL}^{-1}$  HSA solution or 100% HS were used to associate with the HER2-overexpressing SK-OV-3 human ovary cancer cell line, which can be effectively targeted by free anti-HER2-Afb (Figure S4). The SK-OV-3 cells were incubated with the particles at 37  $^{\circ}\text{C}$  for 2 h with a particle-to-cell ratio of 100:1 in serum free McCoy's 5A medium and assessed using deconvolution fluorescence microscopy. Strikingly, the SK-OV-3 cells associated

with a large number of HSA-coated PMA-PEG-Anti-HER2-Afb particles, which was similar to what was observed with these particles without a corona (Figure 3a,b). However, PMA-PEG-Anti-HER2-Afb particles with a protein corona derived from 100% HS showed negligible association to SK-OV-3 cells (Figure 3c).

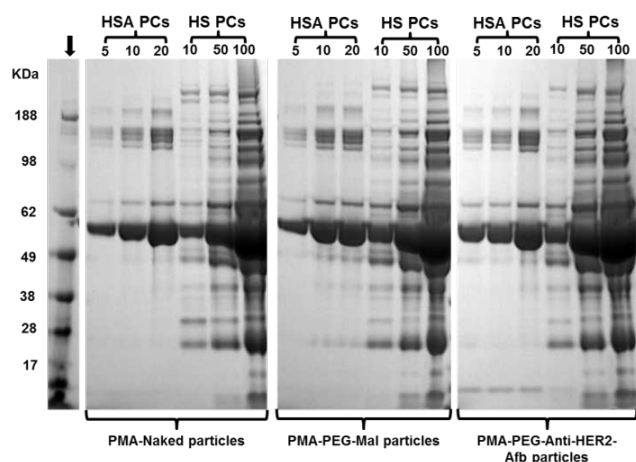


**Figure 2.** SDS-PAGE images of separated corona proteins of the non-functionalized PMA (PMA-Naked) particles, Mal-PEG-Az linker-functionalized PMA (PMA-PEG-Mal) particles, and PMA-PEG-Anti-HER2-Afb particles following incubation for 1 h at 37 °C in media containing different types of proteins at varying concentrations (5, 10, and 20 mg mL<sup>-1</sup> HSA or 10, 50, 100% (v/v) HS). Reference bands associated with particular molecular weights are displayed in the image (as indicated by arrow). “HSA PCs” denotes protein coronas derived from HSA solutions (5, 10, and 20 mg mL<sup>-1</sup>); “HS PCs” denotes protein coronas derived from HS (10, 50, and 100%).

Flow cytometry was employed to quantitatively analyze the association of particles with various protein coronas to the SK-OV-3 cells (Figure 4a,b). Without a protein corona, the PMA-PEG-Anti-HER2-Afb particles express a nearly two-fold higher association to SK-OV-3 cells compared with the PMA-Naked particles or the PMA-PEG-Mal particles, demonstrating the targeting ability of anti-HER2-Afb on the surface of PMA particles. PMA-Naked particles, which were used as a negative control, with protein coronas derived from HSA solutions, did not show significant differences upon association with SK-OV-3 cells compared with particles without a protein corona (Figure 4a). This suggests that the HSA adsorbed on the surface of the particles does not provide additional binding partners to the SK-OV-3 cells by itself. The PMA-PEG-Anti-HER2-Afb particles with protein coronas derived from HSA solutions at various concentrations showed even higher association to SK-OV-3 cells compared with the non-corona coated particles (Figure 4a). However, with protein coronas derived from HS at various concentrations, the PMA-PEG-Anti-HER2-Afb particles dramatically lost their targeting ability as the concentration of HS increased (Figure 4b).

It has been reported that the loss of targeting could be caused by blocked ligand-receptor interaction in the presence of serum proteins.<sup>7</sup> Hence, the interaction between Afb on the surface of particles and its specific receptor was analyzed in the presence of protein coronas. The accessibility of anti-HER2-Afb molecules on particle surfaces was assessed with flow cytometry using fluorescently-labeled anti-Afb IgG. Afb molecules on the surface of particles with HSA coronas exhib-

ited higher accessibility for IgG-binding than particles without a corona (Figure S5a). However, the accessibility of Afb molecules on particles with HS protein coronas decreased significantly (when compared with the non-corona-coated particles) (Figure S5b). This, which is in agreement with the cell association results, indicates that the targeting ability of PMA-PEG-Anti-HER2-Afb particles is directly related to the amount of Afb that is accessible and free to interact with the surrounding environment (and either bind to the HER2 target receptor on cell surface or have anti-Afb-IgG bind to them). With a HSA coating, the ligand-receptor interactions appear to be facilitated, which causes enhanced particle-cell interactions for the functionalized particles. A likely explanation for this is that other components adsorbed by particles from HS inhibited the ligand-receptor interactions, which led to the observed reduction of particle-cell association.

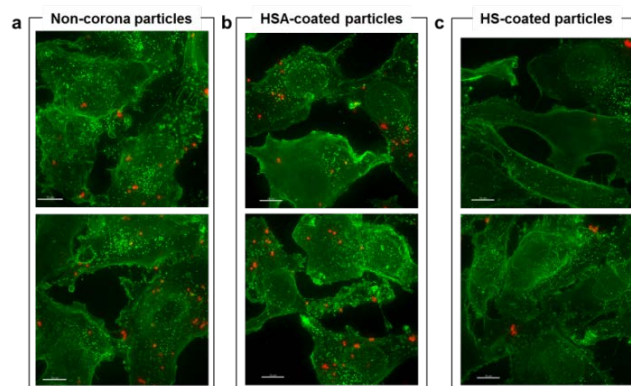


**Figure 3.** Deconvolution microscopy images of SK-OV-3 cells associated with the PMA-PEG-Anti-HER2-Afb particles without a protein corona (a) or with a protein corona derived from 20 mg mL<sup>-1</sup> HSA solutions (b) or 100% HS (c). Cells were incubated with the particles at 37 °C for 2 h at a particle-to-cell ratio of 100:1 in serum-free medium and imaged using deconvolution microscopy after extensive washing in DPBS. The cell membrane was stained with Alexa Fluor 488-conjugated wheat germ agglutinin (WGA488, green), and the particles were labeled with AF633 (labeled to PMA, red). Scale bars are 10 μm.

Another factor which has been reported to influence the cellular interactions of particles is their surface charge.<sup>32,33</sup> Thus, the  $\zeta$ -potential of particles coated with protein coronas from various sources was assessed (in 5 mM phosphate buffer at pH 7.4). The HSA coronas did not cause significant  $\zeta$ -potential changes in any of the particles with different functional groups on their surfaces (Figure 4c). However, the particles with similar overall surface charge showed different particle-cell association trends in the presence of HSA coronas on their surfaces (Figure 4a). Moreover, the adsorption of proteins from HS at various concentrations significantly neutralized the surface charge of the particles (Figure 4d). With the reduction of surface charge, the cell association ability was dramatically reduced for both the Afb-functionalized and non-Afb-functionalized particles (Figure 4b). These observations suggest that various serum proteins other than HSA were adsorbed on the particle surface and form a crucial part of the protein corona. This is further supported by our previous study in which tens of different proteins, from the protein coronas on the surface of functionalized PMA particles, were detected by mass spectrometry.<sup>9</sup> In addition, the neutralization of surface charge via the adsorption of serum proteins may be part of the reason for the reduction in cell association of the particles.

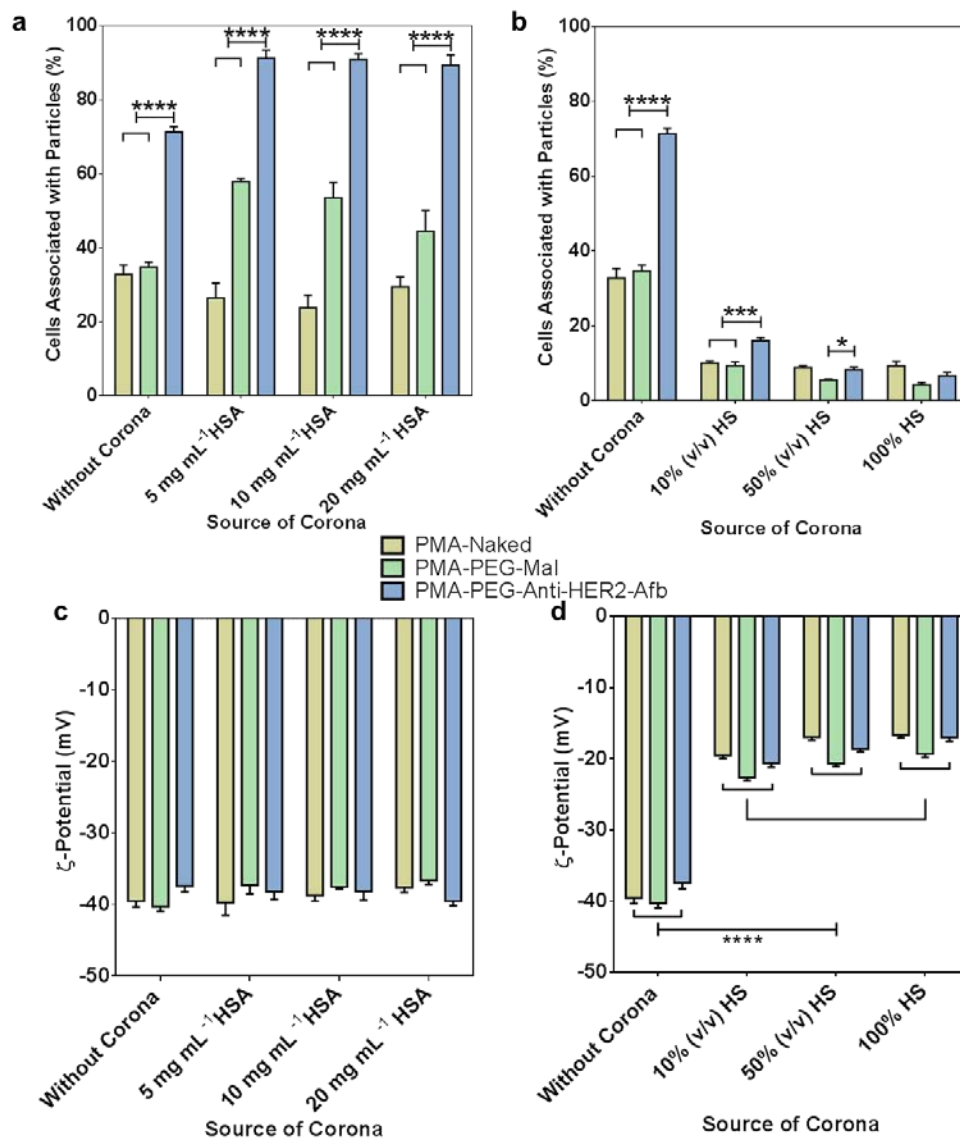


**Figure 4.** a, b) Cell association of AF633-labeled PMA particles to SK-OV-3 cells in the presence of various protein coronas derived from HSA solutions (a) or media containing HS (b) at different concentrations. Data are shown as the mean  $\pm$  standard error of at least four independent experiments, with at least 10 000 cells analyzed in each experiment. c, d)  $\zeta$ -Potential of PMA particles without the protein corona or with protein coronas derived from HSA (c) or HS (d). \*  $p < 0.05$ ; \*\*\*  $p < 0.001$ ; \*\*\*\*  $p < 0.0001$ .

In conclusion, we have demonstrated the different effects of protein coronas on the targeting ability of functionalized particles. Adsorption of HSA alone, the most abundant protein in HS, has shown a favorable effect on facilitating ligand-receptor interactions, resulting in an enhanced targeting ability of Afb-functionalized polymer particles. On the contrary, adsorption of many types of serum proteins dramatically altered the surface properties of the particles, most likely by decreasing the accessibility of conjugated targeting molecules and reducing the surface charge of the particles, which led to the loss of targeting ability of the functionalized particles. Our data therefore highlight the importance of using multicomponent biologically relevant sources of protein coronas (e.g., human serum or human plasma) rather than a single model protein (e.g., albumin). Even though the latter is easier and better defined, it can produce different, or even opposite, results compared with more complex biological solutions. Taken together, this study demonstrates that the type of protein corona influences the targeting ability of particles, and emphasizes

the need for more detailed studies for understanding their targeting ability in the presence of protein coronas, and how to exploit this effect in biological systems.

## ASSOCIATED CONTENT

### Supporting Information.

Experimental methods, materials, and supplementary figures. This material is available free of charge via the Internet at <http://pubs.acs.org>.

## AUTHOR INFORMATION

### Corresponding Author

\* E-mail: [fcaruso@unimelb.edu.au](mailto:fcaruso@unimelb.edu.au).

### Notes

The authors declare no competing financial interest.

## ACKNOWLEDGMENT

This research was conducted and funded by the Australian Research Council Centre of Excellence in Convergent Bio-Nano Science and Technology (project number CE140100036). This work was also supported by the Australian Research Council under the Australian Laureate Fellowship (F.C., FL120100030) and Discovery Early Career Researcher Award (Y.Y., DE130100488) schemes. Q.D. acknowledges funding from the Australian Government through an International Postgraduate Research Scholarship and an Australian Postgraduate Award. This work was performed in part at the Materials Characterisation and Fabrication Platform (MCFP) at The University of Melbourne and the Victorian Node of the Australian National Fabrication Facility (ANFF).

## REFERENCES

1. Choi, C. H.; Alabi, C. A.; Webster, P.; Davis, M. E. *Proc. Natl. Acad. Sci. U.S.A.* **2010**, *107*, 1235-1240.
2. Santra, S.; Kaittanis, C.; Grimm, J.; Perez, J. M. *Small* **2009**, *5*, 1862-1868.
3. Kamphuis, M. M. J.; Johnston, A. P. R.; Such, G. K.; Dam, H. H.; Evans, R. A.; Scott, A. M.; Nice, E. C.; Heath, J. K.; Caruso, F. *J. Am. Chem. Soc.* **2010**, *132*, 15881-15883.
4. Walkey, C. D.; Chan, W. C. W. *Chem. Soc. Rev.* **2012**, *41*, 2780-2799.
5. Monopoli, M. P.; Aberg, C.; Salvati, A.; Dawson, K. A. *Nat. Nanotechnol.* **2012**, *7*, 779-786.
6. Mirshafiee, V.; Mahmoudi, M.; Lou, K. Y.; Cheng, J. J.; Kraft, M. L. *Chem. Commun.* **2013**, *49*, 2557-2559.
7. Salvati, A.; Pitek, A. S.; Monopoli, M. P.; Prapainop, K.; Bombelli, F. B.; Hristov, D. R.; Kelly, P. M.; Aberg, C.; Mahon, E.; Dawson, K. A. *Nat. Nanotechnol.* **2013**, *8*, 137-143.
8. Zarschler, K.; Prapainop, K.; Mahon, E.; Rocks, L.; Bramini, M.; Kelly, P. M.; Stephan, H.; Dawson, K. A. *Nanoscale* **2014**, *6*, 6046-6056.
9. Dai, Q.; Yan, Y.; Ang, C. S.; Kempe, K.; Kamphuis, M. M. J.; Dodds, S. J.; Caruso, F. *ACS Nano* **2015**, *9*, 2876-2885.
10. Fanali, G.; di Masi, A.; Trezza, V.; Marino, M.; Fasano, M.; Ascenzi, P. *Mol. Aspects Med.* **2012**, *33*, 209-290.
11. Fasano, M.; Curry, S.; Terreno, E.; Galliano, M.; Fanali, G.; Narciso, P.; Notari, S.; Ascenzi, P. *IUBMB Life* **2005**, *57*, 787-796.
12. Xu, X.; Qian, Y.; Wu, P.; Zhang, H.; Cai, C. *J. Colloid Interf. Sci.* **2015**, *445*, 102-111.
13. Elsadek, B.; Kratz, F. *J. Control. Release* **2012**, *157*, 4-28.
14. Ramezani, F.; Rafii-Tabar, H. *Mol. Biosyst.* **2015**, *11*, 454-462.
15. Saptarshi, S. R.; Duschl, A.; Lopata, A. L. *J. Nanobiotechnol.* **2013**, *11*, 26.
16. Cedervall, T.; Lynch, I.; Lindman, S.; Berggard, T.; Thulin, E.; Nilsson, H.; Dawson, K. A.; Linse, S. *Proc. Natl. Acad. Sci. U.S.A.* **2007**, *104*, 2050-2055.
17. Yang, L.; Mao, H.; Wang, Y. A.; Cao, Z.; Peng, X.; Wang, X.; Duan, H.; Ni, C.; Yuan, Q.; Adams, G.; Smith, M. Q.; Wood, W. C.; Gao, X.; Nie, S. *Small* **2009**, *5*, 235-243.
18. Vincent, A.; Babu, S.; Heckert, E.; Dowding, J.; Hirst, S. M.; Inerbaev, T. M.; Self, W. T.; Reilly, C. M.; Masunov, A. E.; Rahman, T. S.; Seal, S. *ACS Nano* **2009**, *3*, 1203-1211.
19. Sykes, E. A.; Chen, J.; Zheng, G.; Chan, W. C. *ACS Nano* **2014**, *8*, 5696-5706.
20. Yang, G.; Wang, J.; Wang, Y.; Li, L.; Guo, X.; Zhou, S. *ACS Nano* **2015**, *9*, 1161-1174.
21. Stachler, M. D.; Chen, I.; Ting, A. Y.; Bartlett, J. S. *Mol. Ther.* **2008**, *16*, 1467-1473.
22. Shahin, M.; Ahmed, S.; Kaur, K.; Lavasanifar, A. *Biomaterials* **2011**, *32*, 5123-5133.
23. Stephanopoulos, N.; Tong, G. J.; Hsiao, S. C.; Francis, M. B. *ACS Nano* **2010**, *4*, 6014-6020.
24. Garcia, I.; Sanchez-Iglesias, A.; Henriksen-Lacey, M.; Grzelczak, M.; Penades, S.; Liz-Marzan, L. M. *J. Am. Chem. Soc.* **2015**, *137*, 3686-3692.
25. Ståhl, S.; Kronqvist, N.; Jonsson, A.; Löfblom, J. *J. Chem. Technol. Biotechnol.* **2013**, *88*, 25-38.
26. Nilvebrant, J.; Åstrand, M.; Georgieva-Kotseva, M.; Björnmalm, M.; Löfblom, J.; Hober, S. *Plos One* **2014**, *9*, e103094.
27. Feldwisch, J.; Tolmachev, V. *Methods Mol. Biol.* **2012**, *899*, 103-126.
28. Orlova, A.; Magnusson, M.; Eriksson, T. L. J.; Nilsson, M.; Larsson, B.; Hoiden-Guthenberg, I.; Widstrom, C.; Carlsson, J.; Tolmachev, V.; Stahl, S.; Nilsson, F. Y. *Cancer Res.* **2006**, *66*, 4339-4348.
29. Baselga, J.; Swain, S. M. *Nat. Rev. Cancer* **2009**, *9*, 463-475.
30. Yan, Y.; Björnmalm, M.; Caruso, F. *Chem. Mater.* **2014**, *26*, 452-460.
31. *Harmonisation of Reference Intervals*. Pathology Harmony Group, Clinical Biochemistry Outcomes: UK, January 2011.
32. Fröhlich, E. *Int. J. Nanomed.* **2012**, *7*, 5577-5591.
33. Morachis, J. M.; Mahmoud, E. A.; Almutairi, A. *Pharmacol. Rev.* **2012**, *64*, 505-519.

